ANNALS OF PHYSICS: 21, 72–98 (1963)

Flow of Liquid He II under Large Temperature and Pressure Gradients*

P. P. CRAIG,† W. E. KELLER, AND E. F. HAMMEL, JR.

Los Alamos Scientific Laboratory, University of California, Los Alamos, New Mexico

Two previous papers from this laboratory have reported measurements of heat conduction and fountain pressure for liquid He II flowing through narrow slits ($0.3\mu < d < 3.3\mu$) for temperature differences as large as 1°K. For the lower, yet appreciable, temperature differences the linear two-fluid equations of London and Zilsel were quantitatively verified; integration over the temperature interval was required. The present paper extends the analysis of the measurements to still larger ΔT's, for which the linear equations are no longer applicable. For this purpose integrated solutions of the Gorter-Mellink nonlinear thermohydrodynamic equations, based on the concept of mutual friction, are derived with special emphasis placed on the assumptions and restrictions necessitated by the model. The integrals for heat flow and fountain pressure have been solved numerically using a high-speed computer and the results are compared with the experiments. When Vinen's values of the mutual friction parameter $A(T)$ are employed in the solutions, the comparison is quite good, except near the λ-point; it is also shown that other values of $A(T)$ are not compatible with the observations. An explanation in terms of the vortex line model is proposed for the deviations near T_λ. Despite the agreement between the vortex line theory and experiment obtained here, several as yet unresolved difficulties are associated with flow phenomena in small slits; certain aspects of these problems are discussed, most notably the criteria for the onset of the nonlinear dissipation effects.

I. INTRODUCTION

Experimental studies, designed to test the linear equations of motion for liquid He II under conditions of large temperature and pressure differences in narrow channels of carefully chosen geometry, have been reported in two previous papers (*1*, *2*) (henceforth denoted as I and II). In interpreting these measurements it was necessary to integrate the linear equations of motion over the temperature differences encompassed by the experiments. This approach proved adequate to explain observations on both fountain pressure and heat flow over a far wider range of temperature differences than could be accounted for by the

* Work performed under the auspices of the United States Atomic Energy Commission.
† Now at Brookhaven National Laboratory, Upton, L. I., New York.

ırge Temperature and
dients*

ND E. F. HAMMEL, JR.

sity of California, Los Alamos,
o

y have reported measurements of
quid He II flowing through narrow
fferences as large as 1°K. For the
ices the linear two-fluid equations
erified; integration over the tem-
paper extends the analysis of the
the linear equations are no longer
utions of the Gorter-Mellink non-
ed on the concept of mutual fric-
ed on the assumptions and restric-
grals for heat flow and fountain
ıg a high-speed computer and the
When Vinen's values of the mutual
solutions, the comparison is quite
own that other values of $A(T)$ are
explanation in terms of the vortex
near T_λ. Despite the agreement
nent obtained here, several as yet
low phenomena in small slits; cer-
l, most notably the criteria for the

TION

the linear equations of motion for
perature and pressure differences in
try, have been reported in two pre-
and II). In interpreting these meas-
linear equations of motion over the
experiments. This approach proved
untain pressure and heat flow over a
than could be accounted for by the

nited States Atomic Energy Commission.
pton, L. I., New York.

linearized nonintegrated theory. However, at sufficiently high heat flows saturation effects appeared producing significant deviations from the predictions of the linear theory.

In this paper we shall discuss the relationship of measurements involving very large heat current densities to solutions of the Gorter-Mellink (*3*) nonlinear thermohydrodynamical equations. The integrated nonlinear equations are found to reduce to the linear equations for small heat flows. For larger heat currents the calculations using Vinen's (*4*) values of $A(T)$ in the mutual friction term are in good quantitative agreement with the observations, except in the neighborhood of the λ-point. However, since the Vinen model of dissipation in He II resulting from vortex line turbulence in the superfluid as applied to the present experimental arrangement predicts the breakdown of the equations near the λ-point, the observed deviations may be considered as qualitative support for the theory.

II. DERIVATION OF INTEGRATED FLOW EQUATIONS

A. Derivation of ∇P and ∇T

In order to obtain solutions to the thermohydrodynamic equations of motion for He II which are applicable to long narrow slits and capillaries, we begin with the following two-fluid equations of motion, including mutual friction[1]:

$$\rho_s \frac{D\mathbf{v}_s}{Dt} = -\left(\frac{\rho_s}{\rho}\right)\nabla P + \rho_s s \nabla T - \mathbf{F}_{sn} \tag{1}$$

$$\rho_n \frac{D\mathbf{v}_n}{Dt} = -\left(\frac{\rho_n}{\rho}\right)\nabla P - \rho_s s \nabla T + \mathbf{F}_{sn} - \eta_n \nabla \times \nabla \times \mathbf{v}_n + (2\eta_n + \eta')\nabla(\nabla\cdot\mathbf{v}_n) \tag{2}$$

where

$$\frac{D\mathbf{v}}{Dt} = \frac{\partial \mathbf{v}}{\partial t} + (\mathbf{v}\cdot\nabla)\mathbf{v}.$$

Here the subscripts s and n refer to the superfluid and the normal fluid, η_n is the normal fluid viscosity, and η' is the bulk or second viscosity. The frictional force $\mathbf{F}_{sn}$ accounts for interaction between the superfluid and the normal fluid. The form of this term will be discussed later. Possible other forces acting separately on the normal fluid and on the superfluid are neglected in this treatment.

[1] The equations of motion have been written in various forms, and the correct form for large velocities and including irreversible processes is still controversial. Equations (1) and (2) originate from the ideas of Tisza (*5*), Landau (*6*), London (*7*), and Gorter and Mellink (*3*), and are believed to serve the present purposes well to a good first approximation. The more detailed treatment of the second viscosity terms by Khalatnikov (*8*) is necessary for analyzing experiments on such phenomena as first and second sound; but in experiments on fountain pressure and heat conduction the second viscosity plays a subordinate role and the following more easily handled equations suffice.

In addition to the equations of motion we have conservation of mass

$$\nabla\cdot(\rho_s \mathbf{v}_s + \rho_n \mathbf{v}_n) + \frac{\partial \rho}{\partial t} = 0,$$

and in the counterflow experiments to be discussed the total momentum also vanishes

$$\rho_s \bar{\mathbf{v}}_s + \rho_n \bar{\mathbf{v}}_n = 0, \tag{3}$$

where the bars denote averaging across the slit width.

In steady state flow local accelerations vanish so on the left side of (1) and (2) only the second order terms remain. Adding (1) and (2) we get

$$\begin{aligned}\rho_s(\mathbf{v}_s\cdot\nabla)\mathbf{v}_s + \rho_n(\mathbf{v}_n\cdot\nabla)\mathbf{v}_n = -\nabla P - \eta_n \nabla\times(\nabla\times\mathbf{v}_n)\\ + (2\eta_n + \eta')\nabla(\nabla\cdot\mathbf{v}_n).\end{aligned} \tag{4}$$

The heat current density $\mathbf{q}$ (watts/cm^2) is carried by the normal fluid such that

$$\mathbf{q} = \rho s T \mathbf{v}_n = \mathbf{v}_n \beta^{-1} \tag{5}$$

where $\beta \equiv (\rho s T)^{-1}$. Since heat is assumed to be conserved, $\nabla\cdot\mathbf{q} = 0$ and

$$\nabla\cdot\mathbf{v}_n = \beta\nabla\cdot\mathbf{q} + \mathbf{q}\cdot\nabla\beta = \mathbf{q}\cdot\nabla\beta. \tag{6}$$

Using the vector identity

$$\nabla\times(\nabla\times\mathbf{v}) = \nabla(\nabla\cdot\mathbf{v}) - \nabla^2\mathbf{v}$$

the terms in (4) involving viscosity may be simplified to give

$$\nabla P = \eta_n\nabla^2(\beta\mathbf{q}) + (\eta_n + \eta')\nabla(\mathbf{q}\cdot\nabla\beta) - \rho_s(\mathbf{v}_s\cdot\nabla)\mathbf{v}_s - \rho_n(\mathbf{v}_n\cdot\nabla)\mathbf{v}_n\,. \tag{7}$$

To solve this equation we now make some assumptions which will later be shown to be valid for long narrow slits. Take the z axis along the length of the slit, and the x axis across the slit. Unit vectors in these directions are $\mathbf{e}_z$ and $\mathbf{e}_x$. We assume that

$$\mathbf{q} = q(x)\mathbf{e}_z \quad \text{and} \quad T = T(z) \tag{8}$$

thereby implying that $\beta = \beta(z)$ and $\eta_n = \eta_n(z)$. We further assume that the second order terms on the right of (7) are small compared to the other terms. Using these assumptions (7) may be separated into x and z components to give[2]

$$\frac{\partial P}{\partial z} = \eta_n\,\beta\,\frac{d^2\mathbf{q}}{dx^2} + (2\eta_n + \eta')\mathbf{q}\,\frac{d^2\beta}{dz^2} \tag{9}$$

[2] Most of the following equations in which the heat current density appears are not vector equations. Nevertheless, for convenience we continue to use the boldface notation $\mathbf{q}$ for this quantity.

and

$$\frac{\partial P}{\partial x} = (\eta_n + \eta') \frac{d\mathbf{q}}{dx} \frac{d\beta}{dz}. \tag{10}$$

Equation (9) may be solved if we assume that the second term on the right is small, i.e.

$$\beta^{-1} \frac{d^2\beta}{dz^2} \ll \frac{\eta_n}{2\eta_n + \eta'} \mathbf{q}^{-1} \frac{d^2\mathbf{q}}{dx^2}. \tag{11}$$

(Justification for this assumption will be given later.) Subject to the condition $\mathbf{q} = 0$ at the slit boundaries $\pm d/2$, the solution for $\mathbf{q}$ is

$$\mathbf{q} = \frac{3}{2} \bar{\mathbf{q}} \left(1 - \frac{4x^2}{d^2}\right). \tag{12}$$

Then the pressure gradient becomes

$$\frac{\partial P}{\partial z} = -\frac{12\eta_n \bar{\mathbf{q}}}{\rho s T d^2}. \tag{13}$$

This last equation is the basis of the so-called Allen-Reekie rule, which specifies that in the limit of small ΔT's the fountain pressure P_f and the heat current density are proportional and that this relationship is independent of the form of $\mathbf{F}_{sn}$. Since the right hand side of (13) is strongly temperature dependent, for larger temperature differences this equation must be integrated to give

$$\Delta P_z = P_f = -\int_{T_0}^{T_1} \frac{12\eta_n \bar{\mathbf{q}}}{\rho s T d^2} \frac{dz}{dT} \, dT. \tag{14}$$

In order to obtain the relationship between P_f and $\bar{\mathbf{q}}$ for large temperature differences it is therefore necessary to obtain an expression for dT/dz as a function of the temperature along the length of the slit. Since the temperature gradient along the slit does depend upon $\mathbf{F}_{sn}$, as will be seen below, it is obvious that the relationship between P_f and $\bar{\mathbf{q}}$ must for large temperature differences also depend upon $\mathbf{F}_{sn}$.

We now wish to find an expression for the temperature gradient. To do so we must postulate a particular form for the frictional force $\mathbf{F}_{sn}$. We shall concentrate our attention upon the Gorter-Mellink type of force, which we shall write in the slightly generalized form

$$\begin{aligned} \mathbf{F}_{sn}(\mathbf{v}_s - \mathbf{v}_n) &= A\rho_s\rho_n(|\mathbf{v}_s - \mathbf{v}_n| - \mathbf{v}_c)^{m-1}(\mathbf{v}_s - \mathbf{v}_n) \qquad & |\mathbf{v}_s - \mathbf{v}_n| > \mathbf{v}_c \\ &= 0 & |\mathbf{v}_s - \mathbf{v}_n| < \mathbf{v}_c. \end{aligned} \tag{15}$$

Here A is the (temperature dependent) Gorter-Mellink coefficient, $\mathbf{v}_c$ is a (possibly temperature dependent) critical velocity, and m has in various experiments been found to lie in the range 3–4. The frictional term acts only when the relative velocity $|\mathbf{v}_s - \mathbf{v}_n|$ exceeds $\mathbf{v}_c$.

The boundary condition applied to the normal fluid in obtaining (12) required that the tangential component of the normal fluid velocity vanish at the slit walls. Since the superfluid component is considered to possess no viscosity no similar boundary condition applies and one must resort to other arguments to determine the superfluid velocity profile. A sufficient condition for this profile to be determined is that there exist an arbitrarily small force, a function of $|\mathbf{v}_s - \mathbf{v}_n|$, acting between the superfluid and the normal fluid. The form of the force is immaterial. Then from (1), assuming a nonvanishing force and neglecting as before the terms on the left, we have

$$\mathbf{F}_{sn}(\mathbf{v}_s - \mathbf{v}_n) = \rho_s s \nabla T - (\rho_s/\rho)\nabla P. \tag{16}$$

Equation (16) may then be solved for $\mathbf{v}_s - \mathbf{v}_n$ in the form

$$\mathbf{v}_s - \mathbf{v}_n = f(T, P). \tag{17}$$

We now average across the slit, making use of the earlier assumptions (justified in Section II, B) that T and P undergo negligible variation across the slit.

$$\overline{\mathbf{v}_s - \mathbf{v}_n} = \frac{1}{d}\int_{-d/2}^{d/2} (\mathbf{v}_s - \mathbf{v}_n)\, dx = \frac{1}{d}\int_{-d/2}^{d/2} f(T, P)\, dx = f(T, P). \tag{18}$$

Therefore we conclude that

$$\overline{\mathbf{v}_s - \mathbf{v}_n} = \mathbf{v}_s - \mathbf{v}_n. \tag{19}$$

The normal fluid velocity profile is given (from (12) using $\mathbf{q} = \beta^{-1}\mathbf{v}_n$) by

$$\mathbf{v}_n = \frac{3}{2}\bar{\mathbf{v}}_n\left(1 - \frac{4x^2}{d^2}\right) \tag{20}$$

and hence from (3) the superfluid velocity profile is

$$\mathbf{v}_s = \bar{\mathbf{v}}_n\left[\frac{3}{2}\left(1 - \frac{4x^2}{d^2}\right) - \frac{\rho}{\rho_s}\right] \tag{21}$$

and the superfluid velocity at the slit walls is

$$(\mathbf{v}_s)_{\text{wall}} = -(\rho/\rho_s)\bar{\mathbf{v}}_n. \tag{22}$$

The superfluid flow is rotational, the curl of the velocity being given by

$$\nabla \times \mathbf{v}_s = (12x/d^2)\bar{\mathbf{v}}_n\mathbf{e}_y. \tag{23}$$

The circulation vector is along the y axis and the circulation is a maximum at the slit walls.

At low velocities it is not clear whether a frictional force exists between the

3–4. The frictional term acts only
eds $\mathbf{v}_c$.
normal fluid in obtaining (12) re-
normal fluid velocity vanish at the
onsidered to possess no viscosity no
must resort to other arguments to
sufficient condition for this profile
bitrarily small force, a function of
l the normal fluid. The form of the
g a nonvanishing force and neglect-

$$- (\rho_s/\rho)\nabla P. \qquad (16)$$

$\mathbf{v}_n$ in the form

$$, P). \qquad (17)$$

of the earlier assumptions (justified
ligible variation across the slit.

$$\int_{-d/2}^{d/2} f(T, P)\, dx = f(T, P). \qquad (18)$$

$$- \mathbf{v}_n . \qquad (19)$$

rom (12) using $\mathbf{q} = \beta^{-1}\mathbf{v}_n$) by

$$\frac{4x^2}{d^2}\Big) \qquad (20)$$

rofile is

$$\frac{4x^2}{d^2}\Big) - \frac{\rho}{\rho_s}\Big] \qquad (21)$$

is

$$/\rho_s)\bar{\mathbf{v}}_n . \qquad (22)$$

f the velocity being given by

$$d^2)\bar{\mathbf{v}}_n \mathbf{e}_y . \qquad (23)$$

nd the circulation is a maximum at

a frictional force exists between the

normal and superfluid. A force of the form (15) vanishes for sufficiently small velocities, and for these low velocities further discussion of the superfluid velocity profile is required. Since the superfluid probably flows entirely without dissipation the most likely flow pattern is one without circulation. This would mean that the velocity is constant across the slit. However, there is no experimental evidence supporting this idea, and as we have just shown even a vanishingly small force is sufficient to produce the profile of (21). The situation is analogous to that which occurs in the flow of fluids about airfoils. The solution for the case of vanishingly small viscosity is qualitatively different from that obtained when the viscosity vanishes identically. For identically zero viscosity circulation cannot be established and zero lift is obtained. For vanishingly small viscosity the Kutta boundary condition on the flow applies, and classical lift occurs. It has been shown that for the flow of pure superfluid He II about an airfoil the lift vanishes at low velocities (*9*), and that therefore in subcritical superfluid flow the viscosity is identically zero. It seems probably that a similar situation obtains in the present case and that at sufficiently low relative velocities the frictional force should vanish identically, the superfluid flow being then truly irrotational. It is of interest to note that, could the superfluid velocity profile be measured in a slit at low velocities, one might determine unequivocally, purely from the qualitative character of the flow, whether this is indeed the case.

The z component of (16) is given by

$$\rho_s\, s\,\frac{\partial T}{\partial z} = \frac{\rho_s}{\rho}\,\frac{\partial P}{\partial z.} + A\rho_s\,\rho_n(|\,\mathbf{v}_s - \mathbf{v}_n\,| - \mathbf{v}_c)^{m-1}(\mathbf{v}_s - \mathbf{v}_n). \qquad (24)$$

Using (19) to replace $(\mathbf{v}_s - \mathbf{v}_n)$ by $\overline{\mathbf{v}_s - \mathbf{v}_n}$ and converting velocity into heat current density with (3) and (5) we obtain from (13) and (24) with $m = 3$

$$\frac{\partial T}{\partial z} = -d^{-2}\Lambda^{-1}\bar{\mathbf{q}}[1 + \alpha d^2(\bar{\mathbf{q}} - \mathbf{q}_c)^2] \qquad (25)$$

where

$$(\bar{\mathbf{q}} - \mathbf{q}_c) = 0 \qquad \bar{\mathbf{q}} < \mathbf{q}_c , \qquad \mathbf{q}_c \equiv \rho_s s T \bar{\mathbf{v}}_c ,$$

$$\Lambda = \frac{(\rho s)^2 T}{12\eta_n}$$

and

$$\alpha = \frac{A(\rho_n/\rho)}{12\eta_n(\rho_s/\rho)^3 s^2 T^2} .$$

For all but the smallest temperature differences (25) must be integrated to obtain $\bar{\mathbf{q}}$ as a function of ΔT between the slit ends. When this is done we have

$$d^2 \int_{T_0}^{T_1} \frac{\Lambda dT}{1 + \alpha d^2(\bar{\mathbf{q}} - \mathbf{q}_c)^2} = -\int_{T_0}^{T_1} \bar{\mathbf{q}} \frac{dz}{dT} dT = \bar{\mathbf{q}} L$$

which when rearranged gives

$$\bar{\mathbf{q}} = \frac{d^2}{L} \int_{T_0}^{T_1} \frac{\Lambda dT}{1 + \alpha d^2(\bar{\mathbf{q}} - \mathbf{q}_c)^2}. \tag{26}$$

Equation (25) provides the relationship for the variation of the temperature gradient along the slit length and may be substituted into (14) to yield

$$P_f = \int_{T_0}^{T_1} \frac{\rho s dT}{1 + \alpha d^2(\bar{\mathbf{q}} - \mathbf{q}_c)^2}. \tag{27}$$

Equations (26) and (27) will be used to obtain comparisons with the experimental results of I and II.

It is to be noted that (26) and (27) may be easily altered in order to arrive at solutions for heat flow and fountain pressure in circular capillaries. For a capillary of radius r and length L, d^2 is merely replaced by $3r^2/2$.

B. Neglected Terms

We show first that the approximation of (11) is a good one. We investigate

$$R_1 = \frac{\beta^{-1}(d^2\beta/dz^2)}{[\eta_n/(2\eta_n + \eta')]\bar{\mathbf{q}}^{-1}(d^2\mathbf{q}/dx^2)} \tag{28}$$

and show that $R_1 \ll 1$. In the temperature range of interest $(1.15° < T < 2.15°\text{K})$, $s/s_\lambda \sim \rho_n/\rho \sim (T/T_\lambda)^n$ where $n \sim 5.6$. Let $T/T_\lambda = \zeta$ and $\beta_\lambda = (\rho s_\lambda T_\lambda)^{-1}$. Then

$$\frac{d\beta}{dz} = -(n+1)\beta_\lambda \, \zeta^{-(n+2)} \frac{d\zeta}{dz} \tag{29}$$

and

$$\begin{aligned} \frac{d^2\beta}{dz^2} &= -(n+1)\beta_\lambda \left[-(n+2)\zeta^{-(n+3)} \left(\frac{d\zeta}{dz}\right)^2 + \zeta^{-(n+2)} \frac{d^2\zeta}{dz^2} \right] \\ &= \frac{(n+1)\beta_\lambda(\bar{\mathbf{q}} + \alpha d^2\bar{\mathbf{q}}^3)[(3n+3)\bar{\mathbf{q}} + \alpha d^2\bar{\mathbf{q}}^3(4n + 5 - 2\zeta^n - 4n\zeta^n)]}{\alpha^4\Lambda^2 T_\lambda^2 \zeta^{(n+3)}} \end{aligned} \tag{30}$$

since from (25), neglecting $\mathbf{q}_c$ for simplicity

$$\frac{d\zeta}{dz} = -\frac{1}{d^2\Lambda T_\lambda} (\bar{\mathbf{q}} + \alpha d^2\bar{\mathbf{q}}^3) \tag{31}$$

and

$$\frac{d^2\zeta}{dz^2} = -\frac{(2n+1)}{\zeta}\left(\frac{d\zeta}{dz}\right)^2 + \frac{\alpha\bar{\mathbf{q}}^3}{\Lambda T_\lambda}\left(\frac{n + 2 - 2\zeta^2 - 4n\zeta^n}{\zeta(1 - \zeta^n)}\right)\frac{d\zeta}{dz}. \tag{32}$$

From (12) and (13) we obtain the other required coefficient:

$$\frac{d^2\mathbf{q}}{dx^2} = -\frac{12\bar{\mathbf{q}}}{d^2}. \tag{33}$$

The work of Khalatnikov (*8*) has indicated that the bulk viscosity may be of the order of ten times the ordinary viscosity, so in estimating an upper limit on R_1 we consider the viscosity term to be $\frac{1}{12}$. Also, the maximum value of $\mathbf{q}$ is $\frac{3}{2}\bar{\mathbf{q}}$. Substituting (30) and (33) into (28) we obtain an expression for R_1 in terms of known or calculable quantities. For $d = 2\mu$ and the maximum $\mathbf{q}$'s encountered in these experiments, Table I presents the maximum value attained by R_1 at several temperatures, from which it is seen that in these experiments $R_1 \ll 1$.

The ratio of the pressure gradients R_p across the slit to those along it may be found from (9) and (10), neglecting the small second term in (9).

$$R_p = \frac{\partial P/\partial x}{\partial P/\partial z} = \left(\frac{\eta_n + \eta'}{\eta_n}\right)\frac{(d\mathbf{q}/dx)(d\beta/dz)}{\beta(d^2\mathbf{q}/dx^2)} \tag{34}$$

Estimates of the maximum values of R_p are also given in Table I and indicate that except for the largest heat flows in the vicinity of the λ-point the pressure gradient across the slit is negligible compared to that along the slit. By virtue of the relation (16) between ∇P and ∇T the same statement may be made for the temperature gradient, indicating the extent of validity for the assumption made in (8) that T is a function of z alone.

The second order terms in (1) and (2) may be shown to be small in the same way. We are concerned with gradients of the energy in the z direction. In (2) we compare the z component of the left hand side with the z component of ∇P:

$$R_E = \frac{\rho_n[\partial(\mathrm{v}_n^2/2)/\partial z]}{(\rho_n/\rho)\partial P/\partial z} = \frac{\rho(d/dz)(\beta^2\bar{\mathbf{q}}^2)}{(24\eta_n\bar{\mathbf{q}})/(\rho s T d^2)}. \tag{35}$$

Since

$$\begin{aligned}\beta^2 &= \beta_\lambda^2\zeta^{-2(n+1)},\\ R_E &\sim (n+1)\rho\beta^3\bar{\mathbf{q}}^2(1 + \alpha d^2\bar{\mathbf{q}}^2).\end{aligned} \tag{36}$$

TABLE I

Maximum Values of the Ratios R_1, R_p, and R_E Corresponding to the Maximum Heat Current Density $\bar{\mathbf{q}}_{max}$ at Several Temperatures for Slit I ($d = 2\,\mu$), $T_0 = 1.1$°K

T(°K)	Λ (watt/cm³ − deg)	α (cm²/watt²)	$\bar{\mathbf{q}}$ (watt/cm²)	R_1	R_p	R_E
1.2	3×10^6	6.9×10^5	10^{-1}	$<10^{-4}$	4×10^{-3}	10^{-3}
1.8	7.3×10^8	5.2×10^5	10	$<10^{-5}$	4×10^{-3}	9×10^{-3}
2.15	3.5×10^9	3.3×10^7	15	$<10^{-6}$	$<10^{-1}$	3×10^{-2}

Using the experimental values of $\bar{\mathbf{q}}_{max}$ we find values of R_E given in Table I which indicate that it is reasonable to neglect the second order terms in the calculations of heat flow and fountain pressure.

In obtaining (6) and (25) two assumptions concerning the flow of heat have been made. The first is that conduction of heat by the ordinary diffusive mechanism is small compared to the conduction by the counterflow mechanism. That this is so may be easily verified by considering the results of Zinovieva (*10*) for the ordinary heat conductivity coefficient; when these are applied to the experimental conditions of I and II the amount of heat carried by the normal diffusive process is found to be several orders of magnitude smaller than that transported by the convection process, even at the largest ΔT's.

The second assumption we have made is that the kinetic energy associated with the flow is small compared to the heat flow by internal convection. The heat introduced by the heater at the hot end of the slit will be conveyed as kinetic energy of flow as well as by normal fluid convection. The total heat supplied by the heater then becomes

$$\bar{\mathbf{q}} = \rho s T \bar{\mathbf{v}}_n + \tfrac{1}{2}\rho_n v_n^2 \bar{\mathbf{v}}_n + \tfrac{1}{2}\rho_s v_s^2 \bar{\mathbf{v}}_s . \tag{37}$$

Making use of the vanishing of momentum and defining $\mathbf{q}_i(z)$ as the heat current due to internal convection at any point z in the slit, i.e., $\mathbf{q}_i(z) = \rho s T \mathbf{v}_n$, we have

$$\bar{\mathbf{q}} = \bar{\mathbf{q}}_i(z)\left[1 + \frac{\rho_n(\rho_n^2 - \rho_s^2)}{2\rho_s^2(\rho s T)}\left(\frac{\bar{\mathbf{q}}_i(z)}{\rho s T}\right)^2\right]. \tag{38}$$

The second term in this expression is small for temperatures above 1.1°K and for the heat currents employed in the experiments under discussion, except in the region very close to the λ-point. At 1.2°K the maximum value of this term is of the order -10^{-6}; at about 1.97°K where $\rho_s = \rho_n$ it is of course zero; and even at 2.1°K it is no more than 10^{-4}. Thus kinetic energy terms cannot appreciably alter the heat flow through the slits.

The final point to be discussed in this section is the influence upon the heat flow of the heat generated by viscous forces through shear. According to the two fluid model the normal fluid behaves as a truly classical fluid with a classical viscosity. The heat generated per unit volume per second by shear may be expressed using the Rayleigh dissipation function Φ in the form used by London (*20*)

$$\Phi = \frac{\eta_n}{2}\sum_{ik}\left(\frac{\partial v_{ni}}{\partial x_k} + \frac{\partial v_{nk}}{\partial x_i}\right)^2 + \eta'(\nabla\cdot\mathbf{v}_n)^2. \tag{39}$$

Using the approximations and assumptions made previously, the dominant term is $\eta_n(\partial v_{nz}/\partial x)^2$. With (20) and (5) Eq. (39) becomes upon averaging across the slit:

$$\Phi = \frac{12\eta_n \bar{\mathbf{v}}_n^2}{d^2} = \frac{\bar{\mathbf{q}}^2}{TAd^2}. \tag{40}$$

The total amount of heat generated in the slit per second through the action of viscous forces may be found by integrating this expression over the volume of the slit:

$$\begin{aligned} \dot{Q}_\Phi &= -\int \Phi\, dV = -\int_0^d \int_0^w \int_0^L \frac{\bar{\mathbf{q}}^2}{TAd^2}\, dx\, dy\, dz = \frac{w}{d}\int_{T_0}^{T} \frac{\bar{\mathbf{q}}^2}{TA}\, \frac{dz}{dT}\, dT \\ &= -\, wd\bar{\mathbf{q}} \int_{T_0}^{T_1} \frac{dT}{T(1 + \alpha d^2 \bar{\mathbf{q}}^2)} \end{aligned} \tag{41}$$

Using (25) and assuming in the first approximation that the heat generated does not appreciably perturb the temperature gradient in the slit.

In the lower temperature range we may neglect $\alpha\, d^2 \bar{\mathbf{q}}^2$ compared with unity and Eq. (41) becomes

$$\dot{Q}_\Phi = -w\, d\bar{\mathbf{q}} \ln T_1/T_0 . \tag{41a}$$

Clearly this term is comparable in magnitude with the total heat $\dot{Q} = w\, d\bar{\mathbf{q}}$ and it would at first sight appear that dissipative processes might appreciably affect the over-all heat transport for a given temperature difference. We shall now show that this is not the case, and that in fact the Rayleigh term is responsible for normal fluid generation resulting in the increase in the normal fluid flux between the hot and the cold ends of the slit.

The average normal fluid flux entering the slit at the hot end of the slit is $\bar{\mathbf{N}}_1 = (\rho_n \bar{\mathbf{v}}_n)_1$ gm/cm^2-sec and that leaving the cold end is $\bar{\mathbf{N}}_0 = (\rho_n \bar{\mathbf{v}}_n)_0$ gm/cm^2-sec. The change in flux is then $\overline{\Delta \mathbf{N}} = (\rho_n \bar{\mathbf{v}}_n)_1 - (\rho_n \bar{\mathbf{v}}_n)_0$ gm/cm^2-sec and we assert that this difference arises from the generation of normal fluid within the slit by viscous forces. The effect of normal fluid generation in the slit may be included in the equation of continuity in the manner suggested by Zilsel (*30*):

$$\frac{\partial \rho_n}{\partial t} + \nabla \cdot \rho_n \mathbf{v}_n = \Gamma \tag{42}$$

where Γ(gm/cm^3-sec) represents the generation term for normal fluid (there is of course an equal sink term for superfluid). In steady state flow the time derivative vanishes, and the total change in normal fluid flux may be found by integrating (42) throughout the slit volume. The heat required to generate Γ is $\Gamma s_\lambda T$ (the lambda point entropy s_λ enters because Γ refers to generation of normal fluid alone rather than fluid of density ρ_n, and the approximation $\rho_n/\rho = s/s_\lambda$, valid in the temperature range of interest, is used). Neglecting for the moment dissipation arising in the Gorter-Mellink term we identify this heat with Φ and obtain using (40)

$$\Gamma = \frac{12(\rho_n/\rho)v_n^{\,2}\eta_n}{sTd^2} \tag{43}$$

Upon integrating Γ along the length of the slit, the total normal fluid flux change within the slit is found:

$$\begin{aligned}\int_{T_0}^{T_1} \Gamma\, dz = \int_{T_0}^{T_1} \Gamma \frac{dz}{dT}\, dT &= -\int_{T_0}^{T_1} \frac{\bar{\mathbf{q}}^2}{T^2 s_\lambda\, \Lambda d^2} \frac{\Lambda d^2}{\bar{\mathbf{q}}}\, dT \\ &= -\frac{\bar{\mathbf{q}}}{s_\lambda}\int_{T_0}^{T_1} \frac{dT}{T^2} = \frac{\bar{\mathbf{q}}}{s_\lambda}\left(\frac{1}{T_1} - \frac{1}{T_0}\right).\end{aligned} \tag{44}$$

However, at any temperature T, $\bar{\mathbf{q}} = \rho s T \bar{\mathbf{v}}_n$, so that (44) may be written

$$\int_{T_0}^{T_1} \Gamma\, dz = \left(\frac{\rho s T \bar{\mathbf{v}}_n}{s_\lambda T}\right)_1 - \left(\frac{\rho s T \bar{\mathbf{v}}_n}{s_\lambda T}\right)_0 = (\rho_n \bar{\mathbf{v}}_n)_1 - (\rho_n \bar{\mathbf{v}}_n)_0 = \overline{\Delta \mathbf{N}}, \tag{45}$$

the change in normal fluid flux per unit area over the length of the slit.

The role of Γ in the two fluid equations of motion has been discussed by Zilsel (*30*), and we may readily show using his equations that the perturbation introduced by the dissipation term is exceedingly small. Thus the Rayleigh dissipation term does not contribute to the heat flux (where its effect would be appreciable) but rather the dissipation present generates normal fluid without appreciably influencing the overall heat transport or temperature gradient.

The term analogous to the Rayleigh term for the Gorter-Mellink force is

$$\Phi_{GM} = A\rho_s\rho_n(|\mathbf{v}_s - \mathbf{v}_n| - \mathbf{v}_c)^2(\mathbf{v}_s - \mathbf{v}_n)^2. \tag{46}$$

When this term is added to the Rayleigh term the total change in momentum flux can be calculated in a manner similar to that used in Eq. (44). The only change introduced occurs in the expression for dT/dz for which Eq. (25) is used. The final result (45) is unchanged, for the terms involving the Gorter-Mellink coefficient A drop out. It is likely that there is no dissipation associated with the Gorter-Mellink term (*31*).

III. NUMERICAL SOLUTION OF FLOW EQUATIONS

To solve the nonlinear integral equation (26) use is made of the fact that for given T_0 and T_1 the average heat current density $\bar{\mathbf{q}}$ through the slit is a constant. Therefore with a fixed T_0 chosen as well as a particular value for $\bar{\mathbf{q}}$ Eq. (26) is integrated numerically out to such a T_1 that equality is obtained. The heat current $\bar{\mathbf{q}}$ is then increased by a small increment, and a new (larger) value for T_1 computed. This procedure is repeated until T_1 reaches T_λ. Thus the entire $\bar{\mathbf{q}}$, T_1 curve is obtained. A new value for T_0 is then selected and the entire process repeated. In this way the family of heat flow curves is generated.

Once $\bar{q}$ is determined as above, the solution may be used directly in the numerical integration of Eq. (27) for the fountain pressure P_f. To obtain P_f in mm Hg, (27) is multiplied by the factor 7500 when the following units are used: $\rho(\text{gm/cm}^3)$, $s(\text{joule/gm-deg})$, Λ (watt/cm^3-deg), and $\alpha(\text{cm}^2/\text{watt}^2)$.

We have integrated (26) and (27) on an IBM 704 calculator for the three slits discussed in I and II. The following input data were used in addition to the dimensional values of the slits: $\eta_n(T)$ was determined from the low power heat conduction measurements (see Fig. 6 of I); values of s were taken from the tables of van Dijk and Durieux (*11*); below 1.7°K ρ_n/ρ was obtained from second sound (*12*) data and the thermodynamic calculations of Bendt *et al.* (*13*)—which are in good agreement up to 1.7°K—whereas above 1.7°K ρ_n/ρ was determined as a smoothed average of these two sets of data plus those of Dash and Taylor (*14*).

Values of the total heat flow $\dot{Q}$ (rather than $\bar{q}$) were computed as well as the fountain pressure P_f. In order to compare the computed values of $\dot{Q}$ with the experimentally measured heat flow it is necessary to include the heat flow through the stainless steel of which the slit is constructed. At low heat flows where the nonlinear Gorter-Mellink term is unimportant, flow of heat across the boundary between the helium and the stainless steel does not affect the total heat conductivity since the flow equations are linear and additivity of the two solutions is rigorously correct (as discussed in I). At higher heat currents where the nonlinear terms in the heat conduction equation are important additivity is certainly not correct. The solution to the simultaneous equations becomes exceedingly complicated even in lower approximations. However, looking at the solutions to the two equations separately (assuming a perfectly insulating wall) we find that in the region where the nonlinear term for the flow in helium is large the contribution from the flow in the stainless steel is small. There is therefore probably very little error in using additivity even in this range, for the stainless steel slit cannot perturb the temperature gradient in the helium very much.

Computed values of the fountain pressure and the heat flow including the stainless steel contribution were presented in printed tabular form and also on punched cards. An automatic point plotter was then used to present the calculations in graphical form for comparison with experiment.

IV. COMPARISON OF EXPERIMENTAL RESULTS WITH CALCULATIONS

Using the results of Sections II and III it is possible to extend beyond the linear region the comparison of the experimental results obtained in papers I and II with theoretical calculations. The objects of such a comparison are first to ascertain whether the data are capable of distinguishing between several theories; then, if so, to determine which theory best fits the data; and finally to

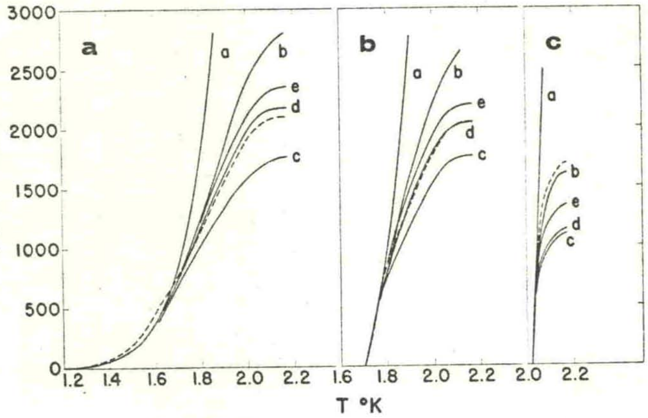

FIG. 1. Comparison of experimental heat flow curves with calculations based on several theories using Eq. (15) and (26); $d = 3.36\ \mu$. a—$T_0 = 1.2°$K; b—$T_0 = 1.7°$K; c—$T_0 = 2.1°$K. Curves a—linear theory ($\alpha\, d^2\bar{q}^2 = 0$); curves b—$m = 3$, $\mathbf{v}_c = 0$, $A = 50$ cm-sec/gm; curves c—$m = 4$, $\mathbf{v}_c = 0$, $A = 50$ cm-sec/gm; curves d—$m = 3$, $\mathbf{v}_c = 0$, A as given by Vinen (*4*); curves e—$m = 3$, $\mathbf{v}_c$ as given by Dash (*16*), A as given by Vinen; ----experimental curves (*1*).

seek plausible explanations for those instances where the "best" theory deviates from the observations.

Examples of the type of theories investigated in the present work and comparison with some experimentally determined heat flows are shown in Fig. 1, where all curves and points refer to Slit III′ (width = 3.36 μ, breadth = 1 cm, and length = 1.9 cm). We recall that the experimental curves are obtained by starting with the cold reservoir in contact with the He bath at some fixed reference temperature, T_0, and then adding successive increments of power $\dot{Q}$ to the thermally isolated reservoir, measuring at each step the equilibrium temperature T_1 attained by the latter reservoir. A heat flow curve is obtained then for given $T_0(\dot{Q} = 0)$ as the variation of T_1 with $\dot{Q}$. Considering first the results for $T_0 = 1.2°$K, Fig. 1a, it is clear that for $T_1 > 1.7°$K the experimental points deviate markedly from the predictions of the linear theory (curve a) and that large correction terms are necessary to describe the observed effects. The Gorter-Mellink force term (Eq. (15)) has been used in a variety of forms in attempts to describe the departure from linearity. The simplest and often used form takes $m = 3$, $\mathbf{v}_c = 0$, and $A = 50$ cm-sec/gm (constant with temperature), although some experiments (e.g. see (*15*)) have indicated that a better fit might be obtained by taking $m = 4$. Curves b and c represent such calculations: curve b with $m = 3$ is seen to be uniformly too high; and curve c with $m = 4$ is uniformly too low. A number of experiments have suggested that A might be temperature dependent and possibly velocity dependent. The first precise measurements yielding values of A vs T are those of Vinen (*4*). The parameter A was found to be a function of temperature and independent of channel size for the large channels used (smallest dimensions of the order of a millimeter). No velocity dependence was found. The heat flow measurements indicated that m should be exactly 3, whereas the effect of $\mathbf{v}_c$ was found for Vinen's system to be unimportant in the equations. In Fig. 1a curve d, obtained using Vinen's values for $A(T)$, $m = 3$ and $\mathbf{v}_c = 0$, shows quantitative agreement with the experimental data. Calculations using (26) and (27) with $\mathbf{v}_c \neq 0$ have been made according to a model in which $\mathbf{v}_c$ is determined at each position z along the slit by a local superfluid critical velocity $\mathbf{v}_{s,c}$ at the wall. By virtue of the equality of $\mathbf{v}_s - \mathbf{v}_n$ and $\bar{\mathbf{v}}_s - \bar{\mathbf{v}}_n$ (Eq. (19)) we have $(\mathbf{v}_{s,c})_{\mathrm{wall}} = \bar{\mathbf{v}}_s - \bar{\mathbf{v}}_n = \mathbf{q}_c/\rho_s sT$. Thus the same relation between $\mathbf{q}_c$ and the critical velocity obtains for a critical superfluid velocity at the wall as for a situation in which the critical velocity occurs in $\bar{\mathbf{v}}_s - \bar{\mathbf{v}}_n$. We have performed calulations for a variation in superfluid velocity with slit width and temperature suggested by Dash (*16*): $\mathbf{v}_c = 0.09\ (\rho_s\, d/\rho)^{-1/2}$ cm/sec when d is given in cm. Curve e in Fig. 1a represents these calculations, which are seen to lie significantly higher than the experimental results.

Figures 1b and 1c show the same comparisons as discussed above for $T_0 = 1.7°$K and 2.1°K respectively. At the former temperature the graph shows again that curve d best represents the experiments, whereas at 2.1°K none of the theories appears adequate. Possible reasons for deviations at temperatures near the λ-point will be discussed later.

Another useful way of testing the various models used in the calculations is to compare their abilities to predict the limiting heat flows at the λ-point. Figure 2 illustrates the ratio of calculated to observed asymptotic heat currents for the various theories for the 3.36 μ slit. Here again it is demonstrated that Vinen's $A(T)$ with no critical velocity provides the best agreement, except for T_0 near T_λ. Since each point on each curve is determined by an entire integration it is not possible to see from this graph alone how agreement might be improved. However, it may be shown that no single value of A can adequately describe the flow for all values of T_0 near the λ-point. Equivalently, this means that in this temperature range A depends upon the heat current present, and that A must be considered to become at high temperatures a function of velocity as well as temperature.

It would be desirable to be able to determine independently and directly from the experimental data the values $A(T)$ which best fit the measurements over the entire range. Unfortunately the results of I and II are not well suited for this purpose, primarily because at the lower temperatures the effect of the Gorter-Mellink term is not large, (i.e., $\alpha\, d^2 \bar{\mathbf{q}}^2 < 1$, hence $\bar{\mathbf{q}}$ is not very sensitive to the precise value of A); and at temperatures near the λ point where it is large A is likely to be velocity dependent, as discussed above. However, it is possible

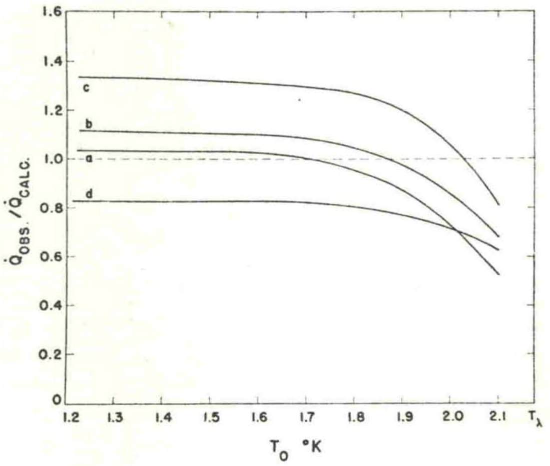

FIG. 2. Ratio of observed asymptotic ($T_1 = T_\lambda$) power input to that calculated on the basis of several theories as a function of T_0 ; $d = 3.36\ \mu$. Curve a—$m = 3$, $\mathbf{v}_c = 0$, A as given by Vinen (*4*); curve b—$m = 3$, $\mathbf{v}_c$ as given by Dash (*16*), A as given by Vinen; curve c—$m = 3$, $\mathbf{v}_c = 0$, $A = 50$ cm-sec/gm; curve d—$m = 4$, $\mathbf{v}_c = 0$, $A = 50$ cm-sec/gm.

to determine a few selected values of A in the region 1.7°–2.0°K for large $\bar{\mathbf{q}}$ where neither of these objections applies. We have not been able to solve the nonlinear integral equation (26) directly for $\bar{\mathbf{q}}$, but instead we have used a variance method pointed out to use by Dr. R. B. Lazarus.

We consider

$$\bar{\mathbf{q}}(\lambda, T) = \frac{d^2}{L}\int_{T_0}^{T} \frac{\Lambda}{1 + \lambda\delta}\, d\tau \tag{44}$$

where $\delta \equiv \alpha d^2 \bar{\mathbf{q}}^2$, $\lambda \equiv \alpha'/\alpha$ is a factor relating α (determined from Vinen's $A(T)$) and α' (the new value of α to be determined from the present experiments); τ is a dummy variable. Holding $\bar{\mathbf{q}}$ fixed and varying λ we obtain

$$0 = \frac{d^2}{L}\left[\frac{\Lambda}{1 + \lambda\delta}\left(\frac{\partial T}{\partial \lambda}\right)_{\bar{\mathbf{q}}} - \int_{T_0}^{T} \frac{\Lambda\delta}{(1 + \lambda\delta)^2}\, d\tau\right]; \tag{45}$$

and holding λ fixed and varying $\bar{\mathbf{q}}$

$$\left(\frac{\partial \bar{\mathbf{q}}}{\partial T}\right)_{\lambda} = \frac{d^2}{L}\left[\frac{\Lambda}{1 + \lambda\delta} - \int_{T_0}^{T} \frac{2\lambda\Lambda\delta}{\bar{\mathbf{q}}(1 + \lambda\delta)^2}\, d\tau \left(\frac{\partial \bar{\mathbf{q}}}{\partial T}\right)_{\lambda}\right]. \tag{46}$$

Combining (45) and (46) we find

$$\left(\frac{\partial T}{\partial \lambda}\right)_{\bar{\mathbf{q}}} = \frac{\bar{\mathbf{q}}}{2\lambda}\left[\left(\frac{\partial T}{\partial \bar{\mathbf{q}}}\right)_{\lambda} - \frac{(1 + \lambda\delta)L}{\Lambda d^2}\right] \tag{47}$$

where all the quantities are to be evaluated at T_1. From the experimental data we compute $(\partial T/\partial \bar{q})_\lambda$ and solve (47) for $(\partial T/\partial \lambda)_{\bar{q}}$ with λ set to unity. Since $\Delta T = (\partial T/\partial \lambda)_{\bar{q}} \Delta\lambda$, where ΔT is the temperature difference at $(T_1, \bar{q})$ between the measured curve and the curve calculated using α (Vinen), we can determine $\Delta\lambda$ and hence $\alpha' = (1 + \Delta\lambda)\alpha$ and new values of A. Table II lists some results of these computations and presents a comparison with values of A as obtained by several other workers. For Slit III′ and $T_1 = 1.800°$, $1.900°$, and $2.000°$K, A has been given for two values of T_0; in each case intermediate values of A would be obtained from heating curves beginning at a temperature between these two limits of T_0. It can be seen from Table II that the experiments are rather well represented by Vinen's values of A. Whereas these considerations may not be useful in any attempt to improve upon Vinen's $A(T)$, it is evident from them that any set of $A(T)$ that is substantially different from those given by Vinen—e.g., as indicated by Brewer and Edwards (*17*) or by Kramers *et al.* (*18*)—would not be compatible with the experiments of I and II.

From the arguments presented above and other comparisons with the data of I and II we have concluded that of the various models we have examined, calculations made using Vinen's $A(T)$, $m = 3$, and $\mathbf{v}_c = 0$ provide the best overall representation for the experimental data for the 3.36 μ and 2.12 μ slits. The general character of the agreement may be observed from an examination of Fig. 3 and 4, where families of the heat flow curves for the 3.36 μ slit are presented as observed and as computed, respectively. A more quantitative comparison for heat flow is presented in Fig. 5, where $[(\dot{Q}_{obs} - \dot{Q}_{calc})/\dot{Q}_{obs}] \times 100$

TABLE II

Comparison of Values of $A(T)$ Obtained from Heating Curves for Slit III′ with Values Obtained by Other Workers

T_1(°K)	T_0(°K) (This work only)	$A(T_1)$(cm sec gm^{-1})			
		Slit III′ $d = 3.36 \times 10^{-4}$ cm	Vinen (*4*) d = 0.4 cm, 0.24 cm	Kramers *et al.* (*18*) d = 0.26 cm	Brewer and Edwards (*17*) d = 0.011 cm, 0.37 cm
1.700	1.083	60 (−7)[a]	75	37[b]	110
1.800	1.083	98 (6)	91	42	140
	1.586	97 (4)			
1.900	1.083	128 (15)	110	52	185
	1.698	117 (5)			
2.000	1.083	150 (20)	135		260
	1.794	111 (−14)			

[a] Numbers in parentheses indicate $(T_{obs} - T_{calc})$ in millidegrees at $(T_1, \bar{q})$.

[b] *Note added in proof:* In the Proceedings of the Eighth International Conference on Low Temperature Physics (London, England, Sept. 16–22, 1962; to be published) Wiarda and Kramers have reported that new measurements of $A(T)$ are in complete agreement with the results of Vinen.

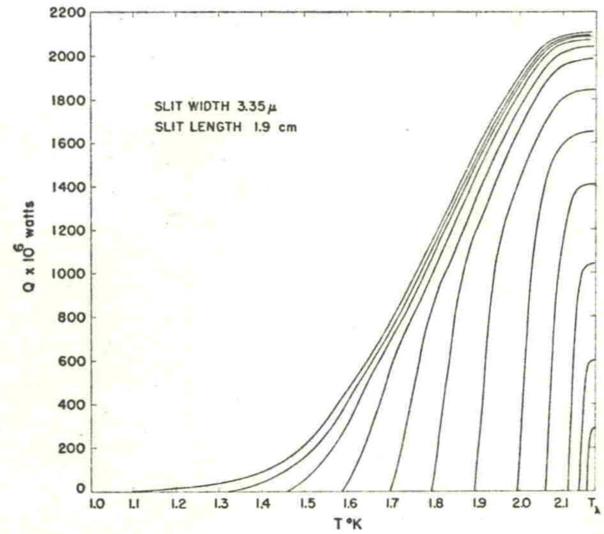

FIG. 3. Family of experimental heat flow curves (*1*); $d = 3.36\ \mu$

is plotted against T_0 for various reduced values $(T_1 - T_0)/(T_\lambda - T_0)$ of the heating curves for both slits. (For Figs. 5 and 6 the experimental curves were graphically interpolated to obtain points at even values of the temperature.) It is seen that the behavior of the two slits is remarkably parallel and that for $T_0 < 1.8°K$ nowhere is the agreement poorer than 20%. Another way of presenting the comparison is shown in Fig. 6 where $[(X_{obs} - X_{calc})/X_{obs}] \times 100$ is plotted against $(T_1 - T_0)/(T_\lambda - T_0)$ for various values of T_0; here X equals either $\dot{Q}$ or P_f, both for the 3.36 μ slit. Generally the fountain pressure calculations exhibit deviations from the experimental results closely similar to those for corresponding heat flow calculations. Although in the regions of $T_0 \leqq 1.3°K$ and low T_1 and of $T_0 > 2.0°K$ and high T_1 the correspondence between the observed $\dot{Q}$ and P_f is somewhat poorer, the calculated fountain pressures nevertheless are in quite good agreement with the measurements. We have already remarked (*2*) upon the low temperature deviations and indicated that the cause most probably does not involve turbulence. The high temperature deviations are discussed in Section V.

The entire discussion thus far has been based on the assumption that the mutual friction force $\mathbf{F}_{sn}(\mathbf{v}_s - \mathbf{v}_n)$ is responsible for the observed nonlinear effects and that such forces as $\mathbf{F}_s(\mathbf{v}_s)$ and $\mathbf{F}_n(\mathbf{v}_n)$, which act on each velocity field independently and which might be included in the equations of motion (1) and (2), are negligible. The conclusion which may be drawn from the data represented in Fig. 6 indicates the validity of this assumption as well as the appli-

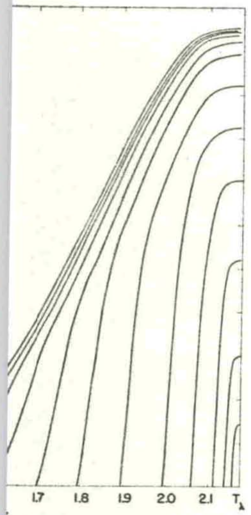

flow curves (1); $d = 3.36\ \mu$

alues $(T_1 - T_0)/(T_\lambda - T_0)$ of the
nd 6 the experimental curves were
even values of the temperature.)
is remarkably parallel and that for
er than 20%. Another way of pre-
where $[(X_{obs} - X_{calc})/X_{obs}] \times 100$
or various values of T_0; here X
lit. Generally the fountain pressure
erimental results closely similar to
s. Although in the regions of $T_0 \leq$
igh T_1 the correspondence between
, the calculated fountain pressures
with the measurements. We have
ature deviations and indicated that
turbulence. The high temperature

based on the assumption that the
onsible for the observed nonlinear
$F_n(v_n)$, which act on each velocity
ded in the equations of motion (1)
may be drawn from the data repre-
is assumption as well as the appli-

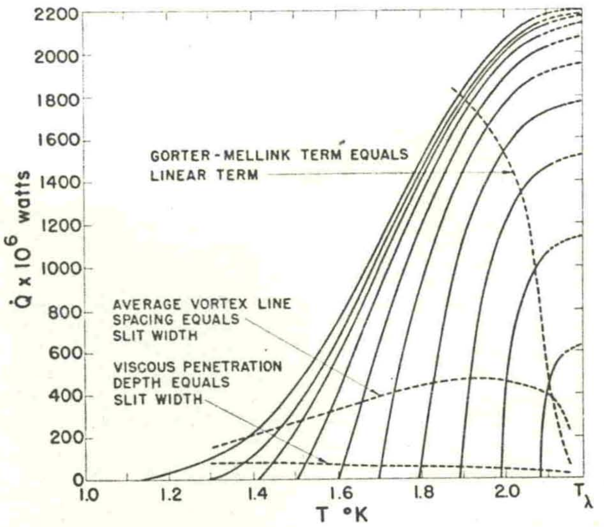

FIG. 4. Family of heat flow curves as calculated using Eq. (26); $d = 3.36\ \mu$, $\mathbf{v}_c = 0$, A as given by Vinen (4). Dashed lines across the heat flow curves indicate several regions useful in interpreting the vortex line model used for the calculations (see Section V).

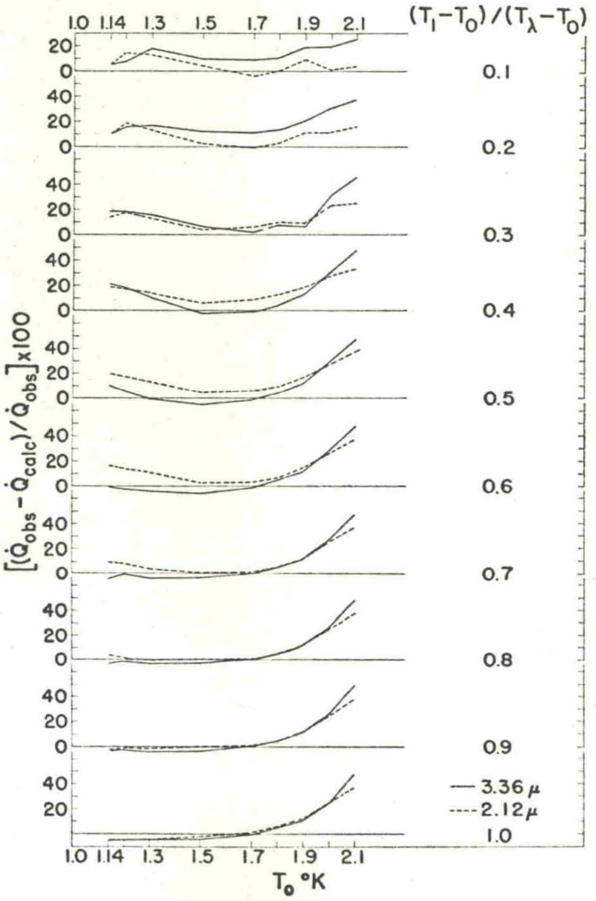

FIG. 5. Percent deviation of calculated heat flow with respect to observed heat flow as a function of initial temperature T_0 for various values of the reduced temperature parameter $(T_1 - T_0)/(T_\lambda - T_0)$; solid curves: $d = 3.36\ \mu$; dashed curves: $d = 2.12\ \mu$.

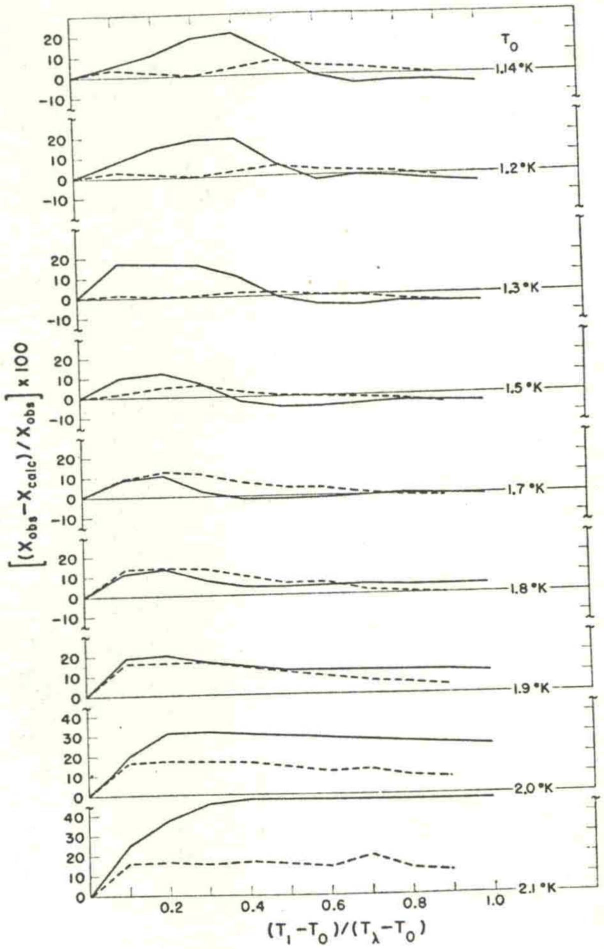

FIG. 6. Percent deviation of calculated heat flow and fountain pressure with respect to the observed quantities as a function of the reduced temperature parameter $(T_1 - T_0)/(T_\lambda - T_0)$ for various values of the initial temperature T_0; $d = 3.36\ \mu$; solid curves: $\mathbf{x}$ = heat flow, $\dot{Q}$; dashed curves: $\mathbf{x}$ = fountain pressure, P_f.

cability of Eq. (14), relating P_f to $\bar{q}$, as determined in the experiments under consideration.

Another way of comparing the character of P_f and that of $\dot{Q}$ is to examine the ΔT (as a function of T_0) at which the experimental points for P_f and $\dot{Q}$ deviate from the linear behavior (denoted by $\Delta T_c = T_1 - T_0$). Figure 7 shows the results for the 3.36 μ slit. For the P_f measurements it is quite clear from Fig. 4 of II that reliable estimates of ΔT_c may be made by visual inspection of the curves. The same is true for $\dot{Q}$ when $T_0 > 1.5°$K (see Fig. 7 of I); for $T_0 <$

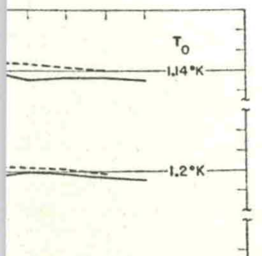

ow and fountain pressure with respect to
uced temperature parameter $(T_1 - T_0)$/
rature T_0 ; $d = 3.36\ \mu$; solid curves: x =
ure, P_f .

etermined in the experiments under

of P_f and that of $\dot{Q}$ is to examine the
rimental points for P_f and $\dot{Q}$ deviate
$T_c = T_1 - T_0$). Figure 7 shows the
urements it is quite clear from Fig. 4
be made by visual inspection of the
> 1.5°K (see Fig. 7 of I); for T_0 <

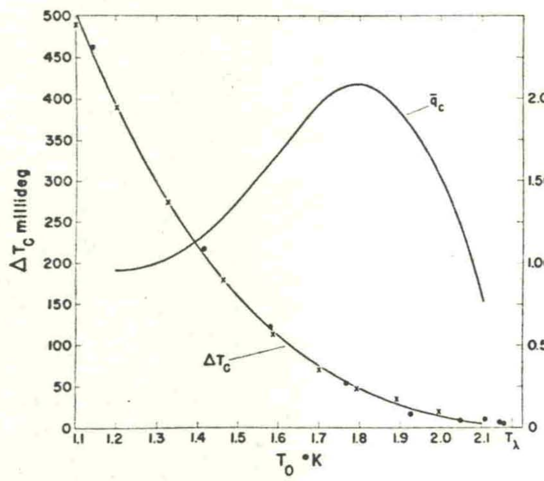

FIG. 7. Critical temperature difference $\Delta T_c = T_1 - T_0$ and corresponding critical heat current density $\bar{q}_c$ as a function of initial temperature T_0 ; $d = 3.36\ \mu$. Solid circles: ΔT_c as obtained from heat flow measurements; crosses: ΔT_c as obtained from fountain pressure measurements; curve for $\bar{q}_c$ obtained from smoothed ΔT_c vs. T_0 curve.

1.5°K ΔT_c has been taken as the inflection point in the curve of $\dot{Q}$ vs. T_1 . From Fig. 7 it is seen that values of ΔT_c as obtained from P_f and $\dot{Q}$ observations determine a single smooth curve as a function of T_0 .

Since it appears that at ΔT_c the character of the flow is modified, we tentatively designate this as the "critical" ΔT, and calculate the corresponding critical heat current density $\bar{q}_c$. The latter is also plotted in Fig. 7 for the 3.36 μ slit. From the smooth curve of $\bar{q}_c$ vs. T_0 we may calculate the average velocities of the two fluids at both the cold end (T_0) and hot end (T_1) of the slit from the relations (3) and (5). The same analysis has been made for the 2.12 μ slit and the results for both channels are given in Table III. Here the subscript c indicates a critical velocity and the superscripts 1 and 0 refer to the hot and cold ends of the slit respectively. A discussion of critical velocities will be given in Section V; but it is interesting to point out here that $\bar{\mathrm{v}}_{s,c}^1$ is generally only slightly greater than $\bar{\mathrm{v}}_{s,c}^0$, indicating that if $\bar{\mathrm{v}}_{s,c}$ is the appropriate critical velocity, the conditions of criticality are achieved along the entire slit length at very nearly a single value of the superfluid velocity. This uniformity of the superfluid velocity along the slit provides some additional justification for the type of critical velocity used in the calculations. It is plausible that should criticality occur at one point of the slit turbulence would be created which would propagate along the entire slit, rather than the condition we have considered of local equilibrium at each point. Since $\bar{\mathrm{v}}_s$ varies but slightly along the slit these two approaches are almost equivalent.

It may at first seem contradictory to derive a critical velocity from the measurements and at the same time to claim the observations are fitted best by a theory which does not include the critical velocity. However, the situation is not as inconsistent as it may appear. As indicated above, $\mathbf{q}_c$ has been determined from the point of first perceptible deviation of the observations from the linear theory; at this point the calculations involving the Gorter-Mellink term with $\mathbf{v}_c = 0$ lie generally about 5% below the experimental data and the linear theory. From the manner in which the observed points deviate from the linear theory it is reasonable to suppose that for $\bar{\mathbf{q}}$ less than $\mathbf{q}_c$ the Gorter-Mellink term does not play a significant role, but that near $\mathbf{q}_c$ the full mutual friction force begins to contribute. For wide slits Vinen has observed a similar behavior and has given a rather detailed discussion of it in relation to the possible existence of "sub-critical" mutual friction (*19*).

In principle the procedure just described for deriving critical velocities from the experimental data ought to be applicable to the computed curves; and it should be possible thereby to obtain graphically values of the "critical velocity" even though the thermohydrodynamical equations used in the calculation do not include critical velocity effects. When we attempt to do this, certain qualitative differences between the calculated and experimental curves emerge rather clearly: whereas in detail the experimental results permit visual recognition of a region in which the character of flow is changing, from which one may infer a critical velocity, the theoretical curves are substantially smoother and a critical velocity does not suggest itself so readily. (A comparison of curves a, d and the dashed line in Fig. 1a illustrate this point nicely.) This is to say that although the theory reproduces the major features of the experimental results, it fails to reproduce the subtleties. Nevertheless, with the aid of reasonable arbitrary criteria we may continue the exercise, the results of which are instructive and perhaps reflect upon an area in which the experimentalist may readily be led astray.

Our prescription for computing $\mathbf{v}_c$ from calculated curves in which no $\mathbf{v}_c$ is used is as follows: For given values of T_0, curves computed with and without inclusion of the Gorter-Mellink term are compared; the heat current corresponding to some arbitrarily chosen deviation of the curves from each other, say 5%, is defined as the "critical heat current"; from this a "critical velocity" may be calculated. Using this prescription results are found in remarkably good agreement with the critical velocities determined from the experimental curves for temperatures below about 1.8°K. However, above 1.8°K the "critical velocity" obtained in this manner falls toward zero, in contrast to the observed values, thereby pointing up the inadequacy of our prescription. Yet the existence of this spurious "critical velocity" criterion may serve as a warning to the experimentalist that care must be exercized in interpreting changes in the character of the solutions of the flow equations in relation to changes in experimentally measured quantities. In passing we note that the criterion used above essentially

e observations are fitted best by a
velocity. However, the situation is
tated above, q_c has been determined
of the observations from the linear
ving the Gorter-Mellink term with
rimental data and the linear theory.
ints deviate from the linear theory
an q_c the Gorter-Mellink term does
the full mutual friction force begins
ved a similar behavior and has given
n to the possible existence of "sub-

for deriving critical velocities from
ble to the computed curves; and it
ally values of the "critical velocity"
quations used in the calculation do
e attempt to do this, certain qualita-
experimental curves emerge rather
results permit visual recognition of a
nging, from which one may infer a
substantially smoother and a critical
A comparison of curves a, d and the
nicely.) This is to say that although
f the experimental results, it fails to
n the aid of reasonable arbitrary cri-
lts of which are instructive and per-
imentalist may readily be led astray.
calculated curves in which no v_c is
curves computed with and without
compared; the heat current corre-
tion of the curves from each other,
rent"; from this a "critical velocity"
results are found in remarkably good
mined from the experimental curves
ver, above 1.8°K the "critical veloc-
ro, in contrast to the observed values,
prescription. Yet the existence of this
serve as a warning to the experi-
nterpreting changes in the character
elation to changes in experimentally
at the criterion used above essentially

requires the term $\alpha\, d^2\bar{q}^2$ occurring in (26) to be of the order of a few percent and that this criterion was in fact suggested earlier by London (*20a*). This requirement implies that $v_c d$ is a function of temperature alone. Such a variation of v_c with slit size has been found to agree with some experiments; but this condition also has only a limited range of applicability and must be considered spurious too.

V. DISCUSSION

In the preceding section we have demonstrated the rather remarkable result that a phenomenological model of the thermohydrodynamic behavior for liquid He II containing no adjustable parameters fits exceedingly well the experimental data obtained for bulk liquid as well as for liquid confined to very narrow channels, over a wide temperature range and for extreme temperature differences. It is significant that to achieve this result it has not been necessary to resort to any detailed, microscopic picture concerning the nature of turbulence in liquid He II. On the other hand we have noted several regions where nontrivial, systematic deviations occur between the measurements and the predictions of the theory. It is believed that at least some of these deviations have their origin in effects associated with the narrowness of the channel widths, and that consideration of a microscopic model is at this point required for a better understanding of the situation. In particular, some of the ideas derived from the Onsager-Feynman quantized vortex-line model appear to be pertinent and may be applied to the present results.

On the assumption that the degeneration of superfluidity in liquid He II comes about from the creation of vortex motion in the superfluid, Vinen has interpreted the mutual friction force in terms of the properties of elementary, quantized vortices. According to Vinen's (*21*) description the Gorter-Mellink coefficient $A(T)$ effectively describes the interactions between the vortex lines, moving with the superfluid, and the thermal excitations comprising the normal fluid. $A(T)$ is calculable from the kinetic model subject to several assumptions and restrictions, among which are two that are of importance when narrow slits are considered: (1) the turbulence is assumed to be homogeneous, requiring that the average distance l between vortex lines is small compared to the smallest dimensions of the slit; and (2) the effective viscous penetration depth, $1/\lambda = 2\eta_n/\rho_n(\bar{v}_n - \bar{v}_s)$, should be small compared to the slit dimensions.

The effect of these restrictions when applied to the calculations for the 3.36 μ slit is indicated in Fig. 4. Values of line spacing in turbulent flow l have been obtained according to Vinen's method from his graph of $l|\bar{v}_s - \bar{v}_n|$ vs. T (Fig. 1 of ref. *21*). It is seen that the viscous penetration depth equals the slit width at smaller relative velocities than does the average vortex line spacing, so that the restriction on the line spacing is the more stringent. Since l decreases as $\bar{q}$

increases $A(T)$ determined from bulk liquid measurements may not be appropriate to the small slits for *any* T_0 at low power inputs. For T_0 less than about 1.8°K this is of little consequence since in that region the experimental data indicate that the contribution of the Gorter-Mellink term is negligibly small when l is large, and becomes appreciable only when $l < d$; however, for T_0 near the λ point this term is important even for low power inputs. Hence, according to Vinen's theory, for the simultaneous conditions of T_0 near T_λ and low $\bar{q}$ we should expect to find poor agreement between theory and experiment, which is indeed the case. Figure 4 also indicates the region in which the Gorter-Mellink term becomes comparable to the linear term. Hence for the larger heat flows the former term dominates and the selection of the proper values of $A(T)$ becomes more important in order to achieve a good fit in this region.

It should be pointed out that near the λ point the vortex-line model as presently developed certainly provides an inadequate description for the very complicated situation of flowing liquid He II; hence the above considerations, although consistent with the theory, probably do not describe the sole mechanism for deviations near the λ point. In section IV we have already mentioned another possible source of deviations, namely, the velocity dependence of the mutual friction force. There are undoubtedly others. Furthermore, the above argument rests upon Vinen's assumption that the degree of turbulence in the fluid is measured by the velocity at a vortex line due to the velocity field of a neighboring line which in turn is assumed to be proportional to the average relative velocity of the two fluids. The validity of this treatment is open to question.

Whereas it is rather reassuring that the results presented here are described so well by the vortex-line theory, it is to be noted that application of this model to the smaller slits ($d < 10^{-3}$ cm) involves certain additional difficulties, some aspects of which are discussed in the following:

The values of the phenomenological parameter $A(T)$ as given by Vinen are by no means generally found by other workers, even for channels with $d > 10^{-3}$ cm. This situation is well summarized by Kramers (*22*), to which may be added data given recently by Brewer and Edwards (*17*). For $d > 10^{-3}$ cm values of $A(T)$ from these other sources show the same temperature dependence as those of Vinen, but differ in magnitude by as much as a factor of ± 2 or 3 (see Table II); for $d < 10^{-3}$ cm some results show the *reverse temperature dependence*. As already indicated $A(T)$ is considered to be descriptive for isotropic turbulence and independent of channel size, except perhaps for "small" channels. Such restrictions being rather vague when applied in practice to a given experimental arrangement, it is not always clear that the experiments are compatible with the assumptions of the theory. With regard to the results of I and II and the present work considerable effort has been made to ascertain whether the theoretical assumptions are satisfied. From the discussion in Section II of this paper

id measurements may not be appro-
power inputs. For T_0 less than about
hat region the experimental data indi-
ellink term is negligibly small when l
en $l < d$; however, for T_0 near the λ
r power inputs. Hence, according to
ons of T_0 near T_λ and low $\bar{q}$ we should
ory and experiment, which is indeed
n in which the Gorter-Mellink term
ence for the larger heat flows the for-
the proper values of $A(T)$ becomes
d fit in this region.
point the vortex-line model as pres-
equate description for the very com-
hence the above considerations, al-
y do not describe the sole mechanism
V we have already mentioned another
velocity dependence of the mutual
rs. Furthermore, the above argument
degree of turbulence in the fluid is
e to the velocity field of a neighboring
ional to the average relative velocity
ment is open to question.
results presented here are described
noted that application of this model
s certain additional difficulties, some
wing:
ameter $A(T)$ as given by Vinen are
cers, even for channels with $d > 10^{-5}$
Kramers (*22*), to which may be added
(*17*). For $d > 10^{-3}$ cm values of $A(T)$
temperature dependence as those of
as a factor of ± 2 or 3 (see Table II);
verse temperature dependence. As al-
descriptive for isotropic turbulence
rhaps for "small" channels. Such re-
l in practice to a given experimental
he experiments are compatible with
d to the results of I and II and the
made to ascertain whether the theo-
discussion in Section II of this paper

and the foregoing remarks about vortex line spacing it appears probable that the conditions are properly met, although the possibility cannot be completely excluded that our agreement with Vinen's findings is partially fortuitous. Further, the possible inadequacy of the theory must be added to the list of uncertainties by taking note of the serious objections to the vortex-line model raised by Lin (*23*) as well as of the conclusion by Townsend (*24*) that a satisfactory description of turbulence in thermal flow of liquid He II is not yet available. Finally, no adequate accounting for wall-effects has been given.

Whereas there still remains considerable divergences in the various experimental measurements concerning the nature of turbulence once it is developed in the flow of liquid He II, there appears to be rather more agreement with respect to determining the point at which turbulence begins. This is not to say that the onset of turbulence at some critical velocity is well understood, nor that such onset is experimentally clear-cut. But it is possible to correlate the critical superfluid velocities obtained from a variety of different types of experiments over a range of eight decades of the characteristic geometric distance, d, associated with the apparatuses used. One such correlation has been given by Atkins (*25*) for $T = 1.4°K$. It can be shown that values of $\bar{v}_{s,c}$ at this temperature obtained from the present work, shown in Table III, are in good accord with the results of other investigators as represented by Atkins' graph.

On the other hand general agreement is not found experimentally for the manner in which $\bar{v}_{s,c}$ depends on temperature for a given geometry. Although several investigations, e.g. those of Staas *et al.* (*26*) and of Winkel *et al.* (*27*), indicate that for 4×10^{-5} cm $< d < 2.6 \times 10^{-2}$ cm $\bar{v}_{s,c}$ passes through a maximum somewhere between 1.5°K and the λ point, the preponderance of evidence suggests that for this range of d, $\bar{v}_{s,c}$ increases with rising temperature. The latter behavior is demonstrated by the measurements from Slits I and III′ listed in Table III. Because of the conflicting experimental results noted above, it is not clear whether $\bar{v}_{s,c}$ becomes large or approaches zero at the λ-point. In this matter, however, some observations made with the smallest channel, Slit II ($d = 0.28\ \mu$), may be helpful. As noted in the earlier papers (I and II) no dissipation effects were evident from the experiments with Slit II, even at very large temperature differences; hence it has not been possible to determine critical velocities for this size channel. However the lowering of the λ-point observed in the fountain pressure measurements appeared to indicate a premature (with respect to temperature) destruction of superfluidity which may be associated with large superfluid velocities near the λ-point. To explain the experimental results an argument consistent with these ideas as well as with those of the vortex model may be constructed as follows: Near T_λ the superfluid fraction becomes relatively small and in order that heat currents of the order of 0.3 watts/cm^2 (as calculated) be maintained the superfluid must flow rather rapidly (>5 cm/

TABLE III

VALUES OF CRITICAL HEAT CURRENT DENSITY $\bar{q}_c$ AND CORRESPONDING FLUID VELOCITIES[a]

	T_0(°K)	T_1(°K)	$\bar{q}_c$ (watt cm^{-2})	$\bar{v}^0_{n,c}$ (cm sec^{-1})	$\bar{v}^0_{s,c}$ (cm sec^{-1})	$\bar{v}^1_{n,c}$ (cm sec^{-1})	$\bar{v}^1_{s,c}$ (cm sec^{-1})
Slit III′ $d = 3.36\ \mu$							
	1.200	1.590	0.96	105	2.9	14.9	2.8
	1.400	1.621	1.15	41.5	3.4	15.7	3.4
	1.600	1.711	1.58	23.5	4.7	15.2	4.9
	1.800	1.847	2.15	15.0	6.8	12.8	7.2
	2.000	2.014	1.53	5.4	7.4	5.3	8.3
	2.100	2.106	0.84	2.2	6.6	2.1	6.8
Slit I $d = 2.12\ \mu$							
	1.400	1.787	2.30	83	6.7	16.8	7.3
	1.600	1.794	2.02	30	6.0	14.3	6.4
	1.800	1.871	1.61	11.3	5.1	8.9	5.7
	2.000	2.037	1.93	6.9	9.5	6.1	10.9
	2.100	2.122	1.54	4.0	12.0	3.7	15.3

[a] The velocities given here are the absolute values averaged over the cross section of the slit assuming laminar flow. The maximum velocity in the channel is then given as $\frac{3}{2}$ times the average velocity. The average relative velocity $\bar{v}_{r,c}$ may be given by $\bar{v}_{s,c} + \bar{v}_{n,c}$. The superscripts 0 and 1 refer to velocities obtained at T_0 and T_1, respectively.

sec). Vortices formed as a result of the flow are associated with the superfluid and are essentially removed from participation in superflow. This effective depletion of the superfluid fraction causes the remaining superfluid to flow more rapidly, thereby creating more vortices. The result is a sort of runaway process which ends in the "self-destruction" of superfluidity through complete conversion to vortex states. From this we would conclude that in small slits the critical velocity does not approach zero at T_λ but remains finite and that $\bar{v}_s$ increases until the superfluid state is suddenly destroyed by the vortex catastrophe. It is not clear at this time whether the same argument may be applied to the results of Atkins *et al.* (*28*) and Seki and Dickson (*29*) who have observed the onset of superfluidity in isothermal flow through channels with $d < 10^{-6}$ cm to be at temperatures considerably below T_λ.

VI. CONCLUSION

Although a number of thermohydrodynamical sets of equations have been applied to the flow of liquid He II, no single set has yet been constructed which completely describes the observed behavior of this quantum liquid. The two-fluid equations including the Gorter-Mellink mutual friction term as interpreted

II

AND CORRESPONDING FLUID VELOCITIES[a]

$\bar{v}^0_{n,c}$ sec^{-1})	$\bar{v}^0_{s,c}$ (cm sec^{-1})	$\bar{v}^1_{n,c}$ (cm sec^{-1})	$\bar{v}^1_{s,c}$ (cm sec^{-1})
05	2.9	14.9	2.8
41.5	3.4	15.7	3.4
23.5	4.7	15.2	4.9
15.0	6.8	12.8	7.2
5.4	7.4	5.3	8.3
2.2	6.6	2.1	6.8
83	6.7	16.8	7.3
30	6.0	14.3	6.4
11.3	5.1	8.9	5.7
6.9	9.5	6.1	10.9
4.0	12.0	3.7	15.3

lues averaged over the cross section of the
ty in the channel is then given as 3/2 times
ocity $\bar{v}_{r,c}$ may be given by $\bar{v}_{s,c} + \bar{v}_{n,c}$.
ined at T_0 and T_1 , respectively.

w are associated with the superfluid
ation in superflow. This effective de-
e remaining superfluid to flow more
e result is a sort of runaway process
perfluidity through complete conver-
onclude that in small slits the critical
remains finite and that $\bar{v}_s$ increases
royed by the vortex catastrophe. It
rgument may be applied to the results
(*29*) who have observed the onset of
channels with $d < 10^{-6}$ cm to be at

USION

namical sets of equations have been
le set has yet been constructed which
or of this quantum liquid. The two-
k mutual friction term as interpreted

on the basis of the vortex line model has been shown by others to represent rather well most of the experimental observations. In the present paper these equations have been applied to the flow of He II through narrow slits and have been tested over a range of temperature and pressure gradients substantially larger than has been studied hitherto. Furthermore, a detailed study has been made of the approximations made in arriving at solutions of the equations of motion as well as of the limitations implied by the vortex line model for superfluid turbulence. Within this framework the agreement found between theory and experiment is generally quite good. In addition the Gorter-Mellink mutual friction coefficient as determined by Vinen for large channels and small temperature gradients has been found to be equally appropriate for narrow channels and large temperature gradients in those regions where the vortex line model indicates it should be valid, and not elsewhere. It would thus appear that the equations used here are applicable over an exceptionally wide range and are capable of describing a broad spectrum of flow phenomena of superfluid helium.

ACKNOWLEDGMENT

The authors wish to express their appreciation to Dr. R. B. Lazarus for helpful discussions and for indicating the variance method used to obtain approximate values of the Gorter-Mellink constant from the experimental data.

REFERENCES

1. W. E. KELLER AND E. F. HAMMEL, JR., *Ann. Phys.* (*N.Y.*) **10**, 202 (1960). (I)
2. E. F. HAMMEL, JR. AND W. E. KELLER, *Phys. Rev.* **124**, 1641 (1961). (II)
3. C. J. GORTER AND J. H. MELLINK, *Physica* **15**, 285 (1949).
4. W. F. VINEN, *Proc. Roy. Soc.* **A240**, 114 (1957).
5. L. TISZA, *Phys. Rev.* **72**, 838 (1947).
6. F. LONDON, *Phys. Rev.* **54**, 947 (1938).
7. L. LANDAU, *J. Phys. U.S.S.R.* **5**, 71 (1941); *ibid.* **11**, 91 (1947).
8. I. M. KHALATNIKOV, *J.E.T.P.* (*U.S.S.R.*) **20**, 243 (1950).
9. P. P. CRAIG AND J. R. PELLAM, *Phys. Rev.* **108**, 1109 (1957).
10. K. N. ZINOVIEVA, *J.E.T.P.* (*U.S.S.R.*) **31**, 31 (1956).
11. H. VAN DIJK AND M. DURIEUX, Helium vapor pressure scale T_{L55} . Kamerlingh Onnes Laboratory, Leiden, Holland (1955).
12. D. DE KLERK, R. P. HUDSON, AND J. R. PELLAM, *Phys. Rev.* **89**, 662 (1953); R. D. MAUER AND M. A. HERLIN, *Phys. Rev.* **76**, 948 (1949); *ibid.* **81**, 444 (1951).
13. P. J. BENDT, R. D. COWAN, AND J. L. YARNELL, *Phys. Rev.* **113**, 1386 (1959).
14. J. G. DASH AND R. D. TAYLOR, *Phys. Rev.* **105**, 7 (1957).
15. D. F. BREWER, D. O. EDWARDS, AND K. MENDELSSOHN, *Phil. Mag.* **1**, 1130 (1956).
16. J. G. DASH, *Phys. Rev.* **94**, 1091 (1954).
17. D. F. BREWER AND D. O. EDWARDS, *Phil. Mag.* **7**, 721 (1962).
18. H. C. KRAMERS, T. M. WIARDA, AND A. BROESE VAN GROENOU, *in* "Proceedings of the Seventh International Conference on Low Temperature Physics," G. M. Graham and A. C. Hollis Hallett, ed., p. 562. Univ. Toronto Press, Toronto, Canada, 1961.
19. W. F. VINEN, *in* "Progress in Low Temperature Physics," C. J. Gorter, ed., Vol. III, p. 44 ff. North Holland Publishing Co., Amsterdam, 1961.

20. F. London, "Superfluids." Vol. 2, p. 86. Wiley, New York, 1954.
20a. F. London, "Superfluids," Vol. 2, p. 163. Wiley, New York, 1954.
21. W. F. Vinen, *Proc. Roy. Soc.* **A242**, 493 (1957).
22. H. C. Kramers, *Physica (Suppl.)* **26**, 581 (1960).
23. C. C. Lin, *in* "Proceedings of the International Summer School of Physics, Varenna, Italy," to be published.
24. A. A. Townsend, *J. Fluid Mech.* **10**, 113 (1960).
25. K. R. Atkins, "Liquid Helium," p. 200. Cambridge Univ. Press, Cambridge, England, 1959.
26. F. A. Staas and K. W. Taconis, *Physica* **27**, 924 (1961).
27. P. Winkel, A. M. G. Delsing, and J. D. Poll, *Physica* **21**, 331 (1955).
28. K. R. Atkins, E. U. Condon, and H. Seki, *Phys. Rev.* **102**, 582 (1956).
29. H. Seki and C. C. Dickson, *in* "Proceedings of the Seventh International Conference on Low Temperature Physics," G. M. Graham and A. C. Hollis Hallett, eds., p. 569. Univ. of Toronto Press, Toronto, Canada, 1961.
30. P. R. Zilsel, *Phys. Rev.* **79**, 309 (1950).
31. H. N. V. Temperley, *Proc. Phys. Soc.* **A64**, 105 (1951).